

Cite this: *Soft Matter*, 2011, **7**, 7375

www.rsc.org/softmatter

PAPER

## Magnetic colloidosomes fabricated by Fe<sub>3</sub>O<sub>4</sub>–SiO<sub>2</sub> hetero-nanorods†

Lu Zhang,<sup>a</sup> Fan Zhang,<sup>a</sup> Ying-Shuai Wang,<sup>a</sup> Yun-Lu Sun,<sup>a</sup> Wen-Fei Dong,<sup>\*a</sup> Jun-Feng Song,<sup>a</sup> Qi-Sheng Huo<sup>b</sup> and Hong-Bo Sun<sup>\*ac</sup>

Received 2nd February 2011, Accepted 10th May 2011

DOI: 10.1039/c1sm05184a

Magnetic colloidosomes were fabricated by directing self-assembly of magnetic-mesoporous hetero-nanorods at the interface of water-in-oil droplets. Emulsions stabilized by the adsorbed particles without any surfactant indicate that such rod-like nanoparticles have specific advantages in making stable and intact shells than spherical particles. The integrity and emulsion stability of the colloidosomes were strongly influenced by the geometric shape of the hetero-nanorods. The optimum length of the nanorods to construct the colloidosomes was studied and demonstrated. The as-formed magnetic colloidosomes can exhibit unique encapsulation behaviors and show strong magnetic response properties, which will find huge potential application in multicompartment reactor, drug delivery and other biomedical fields.

### Introduction

Microencapsulation is of considerable interest for a wide variety of applications and technologies, ranging from functional foods to drug delivery to biomedical applications.<sup>1–4</sup> Various synthetic routes have been developed for fabricating microcapsules which can prevent molecules inside from leaking out and unwanted molecules from diffusing in.<sup>5</sup> In general, microcapsules are usually constructed by emulsion polymerization,<sup>6</sup> crosslinking polymerization,<sup>7</sup> polymer phase separation,<sup>8,9</sup> and electrostatic layer-by-layer deposition,<sup>10,11</sup> etc. Recently, self-assembly of colloidal particles into the interface of emulsion droplets, usually called “Pickering emulsions”, has attracted great attention.<sup>12–18</sup> Velev *et al.* first developed microcapsules by the assembly of polystyrene latex particles around *n*-octanol-in-water emulsion droplets.<sup>13</sup> Then, Dinsmore *et al.* modified the process by thermally fusing the particles in the shell and first described the microcapsules as “colloidosomes”.<sup>12</sup> These shells are dense nanoparticle films with a high permeability owing to the large interstitial voids. Besides organic colloidal particles, numerous functional inorganic nanoparticles (NPs) can be utilized to fabricate smart colloidosomes, *i.e.* magnetic Fe<sub>3</sub>O<sub>4</sub> NPs,<sup>19</sup> catalytic TiO<sub>2</sub> NPs,<sup>20</sup> semiconducting SnO<sub>2</sub> NPs,<sup>21</sup> and biocompatible SiO<sub>2</sub> NPs,<sup>12</sup> etc.

Recently, magnetic colloidosomes have received more attention in biomedical fields, for instance in the delivery and controlled release of antibodies, proteins, drugs, and so on.<sup>22–27</sup> If magnetic colloidosomes have a high magnetization at room temperature, potentially they can be directed towards a specific target in the human body and remain localized using a very low applied magnetic field.<sup>28,29</sup> For this reason, many approaches have been developed to fabricate magnetic colloidosomes. For example, Duan *et al.* fabricated magnetic colloidosomes by directing the self-assembly of magnetite (Fe<sub>3</sub>O<sub>4</sub> NPs) at the interface of water-in-oil droplets.<sup>19</sup> In addition, the Gao group created hollow magnetic capsules using Janus magnetic NPs.<sup>30</sup> However, magnetic colloidosomes made by such small magnetic NPs are not dynamically stable enough and show a relative low magnetic response. In order to overcome these drawbacks, the novel approach of click-mediated crosslinking of NPs at water–oil interfaces have been successfully developed by the Rotello group.<sup>31</sup> Although the stability of as-resulting colloidosomes are highly improved, the polymer synthesis and crosslinking reaction are too complicated to be handled easily. Therefore, a simple, low-cost and rapid fabrication method is necessary.

As demonstrated in our previous work, highly water dispersible magnetite (Fe<sub>3</sub>O<sub>4</sub>) with a uniform size of 100 nm composed of many single magnetite crystallites can be successfully synthesized.<sup>32</sup> The as-formed magnetic particles show superparamagnetic properties at room temperature, whereas a single magnetite particle of the same size would exhibit ferromagnetic behavior. In this work, we aim to develop a magnetic controlled colloidosome system, which can be guided into desired sites and/or retain them at the target site by means of an external magnetic force, by using these magnetic NPs. However, hydrophilic magnetic NPs can not form stable microcapsules at the interface of water-in-oil droplets.

<sup>a</sup>State Key Laboratory on Integrated Optoelectronics, College of Electronic Science and Engineering, Jilin University, 2699 Qianjin Street, Changchun, 130012, P. R. China. E-mail: dongwf@jlu.edu.cn; hbsun@jlu.edu.cn

<sup>b</sup>State Key Laboratory of Inorganic Synthesis and Preparative Chemistry, College of Chemistry, Jilin University, Changchun, 130012, P. R. China

<sup>c</sup>College of Physics, Jilin University, 119 Jiefang Road, Changchun, 130023, P. R. China. E-mail: hbsun@jlu.edu.cn

† Electronic supplementary information (ESI) available. See DOI: 10.1039/c1sm05184a

Increasing hydrophobicity will be helpful to improve the stability of the colloidosomes. Therefore, a thin silica layer will be applied to the particle surfaces in order to control the surface hydrophobicity. In addition, the silica coating will also enhance the biocompatibility of the NPs. In this respect,  $\text{Fe}_3\text{O}_4$ -core/ $\text{SiO}_2$ -shell NPs ( $\text{SiO}_2@ \text{Fe}_3\text{O}_4$ ) and  $\text{Fe}_3\text{O}_4$ - $\text{SiO}_2$  rod-like NPs ( $\text{Fe}_3\text{O}_4$ - $\text{SiO}_2$  hetero-nanorods) have been prepared by using a simple sol-gel method.<sup>33</sup> We found that the spherical  $\text{SiO}_2@ \text{Fe}_3\text{O}_4$  NPs were unable to serve as building blocks for constructing magnetic capsules in the emulsification method (Scheme 1). However, hetero-nanorods can be facily used to prepare surfactant-free magnetic microcapsules. Furthermore, the shape effect on the integrity and stability of the colloidosomes were studied, and their encapsulation and magnetic manipulation properties were investigated in this work.

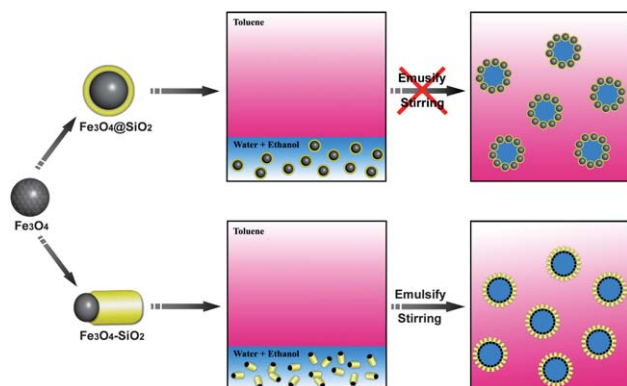
## Experimental methods

### Reagents

Polyacrylic acid (PAA), iron (III) chloride anhydrous ( $\text{FeCl}_3$ ), diethylene glycol (DEG), agarose (for routine use), sodium hydroxide (NaOH), ethanol, ammonium hydroxide ( $\text{NH}_4\text{OH}$ , 28%), cetyltrimethyl-ammonium-bromide (CTAB) and tetraethyl orthosilicate (TEOS, 98%) were purchased from Sigma-Aldrich. All reagents were commercially available products with analytical grade purity and used without further purification.

### Preparation of superparamagnetic NPs

The  $\text{Fe}_3\text{O}_4$  NPs were produced using a high temperature hydrolysis reaction.<sup>34,35</sup> A stock NaOH solution was prepared by dissolving 2.0 g of NaOH in 20 mL of DEG.  $\text{FeCl}_3$  (0.8 mmol), PAA (8 mmol), and DEG (34 mL) were added to a three-necked flask, and the mixed solution was heated to 220 °C for 30 min under nitrogen. The NaOH solution was then dropped rapidly into the mixture with vigorous mechanical stirring for an additional 1 h. The products were washed with deionized water and ethanol *via* centrifugation.



**Scheme 1** Illustration of the process of preparing magnetic colloidosomes based on the self-assembly of  $\text{SiO}_2@ \text{Fe}_3\text{O}_4$  NPs or  $\text{Fe}_3\text{O}_4$ - $\text{SiO}_2$  hetero-nanorods at the interface of toluene and a mixture of water and ethanol.

### Synthesis of $\text{Fe}_3\text{O}_4$ core/ $\text{SiO}_2$ shell NPs

$\text{SiO}_2@ \text{Fe}_3\text{O}_4$  core-shell NPs were prepared through a modified Stöber method.<sup>36</sup> 1 mL  $\text{Fe}_3\text{O}_4$  aqueous solution (8.6 mg  $\text{mL}^{-1}$ ) was mixed with 10 mL ethanol, 0.5 mL ammonium hydroxide aqueous solution and 0.1 mL TEOS, followed by vigorous stirring for 40 min. Products were obtained after washing with ethanol three times.

### Preparation of $\text{Fe}_3\text{O}_4$ - $\text{SiO}_2$ hetero-nanorods<sup>33</sup>

With TEOS as a silica source, CTAB as a template and  $\text{Fe}_3\text{O}_4$  NPs as a substrate, a mesoporous silica stick could be formed on the magnetic sphere. 0.05 g CTAB was dissolved in 10 mL ultrapure water under ultrasonic treatment. 1 mL (8.6 mg  $\text{mL}^{-1}$ )  $\text{Fe}_3\text{O}_4$  NP solution was added to the CTAB solution, then ultrasonic treatment was applied for 30 min. The mixture was mechanically stirred at 40 °C in a water bath and 0.5 mL  $\text{NH}_4\text{OH}$  was injected into the solution, followed by a certain amount of TEOS. After 30 min, magnetic-mesoporous rod-like NPs were obtained and were washed with ethanol three times. The aspect ratio (2 : 1, 3 : 1, 5 : 1 and 7 : 1) of the rod-like NPs could be facily controlled by the molar ratio of  $[\text{TEOS}]/[\text{Fe}_3\text{O}_4 \text{ NP}]$  (3.8, 4.9, 7.6 and 11.3), respectively.

### Preparation of magnetic colloidosomes

0.5 mL  $\text{Fe}_3\text{O}_4$  NP (5 mg) aqueous solution or 0.5 mL magnetic silica ethanol solution containing 5 mg of either  $\text{SiO}_2@ \text{Fe}_3\text{O}_4$  core-shell NPs or  $\text{Fe}_3\text{O}_4$ - $\text{SiO}_2$  rod-like NPs was added to a mixture of a certain amount of aqueous water (0.1–1 mL) and 5 mL toluene. After emulsification by magnetic stirring for 30 min at room temperature, magnetic colloidosomes from water-in-toluene droplets stabilized with dense magnetic particle films, were obtained.

### Characterization

Transmission electron microscopy (TEM) images were taken with a Hitachi H-8100IV Transmission Electron Microscope operated at 200 kV. Magnetic measurements were carried out using a TDM-B vibrating sample magnetometer (VSM) at 300 K. Confocal images were implemented by a Leica confocal laser scanning microscope with a 10× objective. Z-potential measurements were performed using a Zeta sizer NanoZS (Malvern Instruments, USA). Raman spectra were recorded by a OMATS89 Raman spectrometer (JY Company, France).

## Results and discussion

### Self-assembly of $\text{SiO}_2@ \text{Fe}_3\text{O}_4$ core-shell NPs at the interface of water-in-oil droplets

With the development of nanotechnology, more attention has been focused on Pickering emulsions which are the adsorption of nanoparticles at the oil/water interface and the emulsion droplets are stabilized by nanoparticles.<sup>37–40</sup> Herein, our purpose was to develop a novel stable magnetic microcapsule by the self-assembly of magnetic NPs at the droplet surface. At first, the high water-soluble  $\text{Fe}_3\text{O}_4$  NPs were employed as building blocks to construct the colloidosomes. Fig. 1a shows a TEM image of

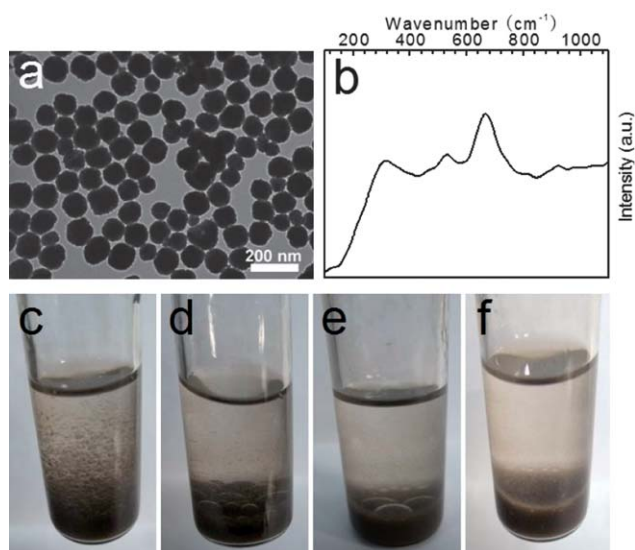


**Fig. 1** TEM image (a) and Raman spectra (b) of  $\text{Fe}_3\text{O}_4$  NPs. (c–f) Photographs of toluene dispersed magnetic capsules consisting of  $\text{Fe}_3\text{O}_4$  NPs. After violent shaking, many small droplets emerged from the emulsion, and the  $\text{Fe}_3\text{O}_4$  NPs were well dispersed in the center of the droplets. Small droplets (c) turned to bigger droplets (d–e) rapidly and all droplets disappeared within 5 s (f).

$\text{Fe}_3\text{O}_4$  NPs, 100 nm in diameter, which are composed of many single magnetite crystallites approximately 10 nm in size.<sup>32</sup> Raman spectra of  $\text{Fe}_3\text{O}_4$  NPs were recorded with a 514 nm argon ion laser as an excitation source (Fig. 1b). There are three clear peaks at 667, 535 and 316  $\text{cm}^{-1}$ , which can be indexed to the  $A_{1g}$ ,  $T_{2g}$  and  $E_g$  modes of the  $\text{Fe}_3\text{O}_4$  NPs, respectively. The NPs are highly hydrophilic since their Zeta potential is  $-49$  mV. Fig. 1c–f shows a series of photographs of the dynamic self-assembly behavior of the  $\text{Fe}_3\text{O}_4$  NPs in a water-toluene mixture. As shown in Fig. 1c, after violent shaking, emulsion droplets spontaneously form in the solution. However, the small droplets were not stable because they would form bigger droplets within 5 s.

Generally, the adsorption of the particles onto the interface of the water/oil droplets appears to be closely related to the charge of the particles.<sup>41,42</sup> In Pickering emulsions, the electrostatic repulsion between the charged particles at the interface increases when the charged particles are stable at the interface of water and low relative permittivity (air or oil).<sup>43,44</sup> Therefore, to construct a stable capsule, the electrical charge of the particles should not be too high. This reason explains why high charged  $\text{Fe}_3\text{O}_4$  NPs cannot migrate at the droplet surfaces.  $\text{Fe}_3\text{O}_4$  particles in the original aqueous suspension are protected from precipitation (caused by van der Waals) by the repulsive electrostatic and hydration forces of the charged carboxylic acid groups on their surfaces. The high negative potential of the particles at the beginning of the process makes the adsorption process impossible, because of the strong electrostatic repulsion and hydration forces.

To induce adsorption of the particles on the oil/water interface, the magnitude of their surface charge needs to be reduced. In this respect, water soluble  $\text{Fe}_3\text{O}_4$  NPs were coated with a thin layer of silica shell in order to decrease the surface charge and increase the hydrophobicity. As shown in Fig. 2, highly uniform

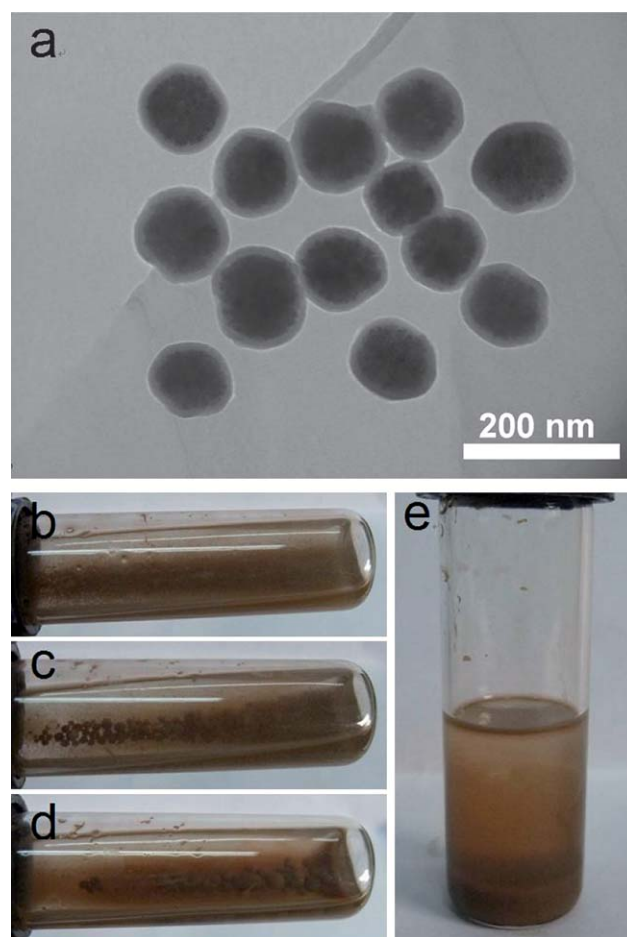


**Fig. 2** (a) TEM image of  $\text{SiO}_2@\text{Fe}_3\text{O}_4$  NPs. (b–e) Photographs of toluene dispersed magnetic capsules consist of  $\text{SiO}_2@\text{Fe}_3\text{O}_4$  NPs. After violent shaking, many small droplets emerged from the emulsion, and the core-shell NPs were well dispersed in the center of droplets. Small droplets (b) turned to big droplets (c,d) until all droplets disappeared after 10 s (e).

and spherical  $\text{SiO}_2@\text{Fe}_3\text{O}_4$  NPs with a controlled silica shell thickness were selected to fabricate colloidosomes. The TEM image in Fig. 2a shows that the core-shell NPs have a 100 nm  $\text{Fe}_3\text{O}_4$  core and 20 nm silica shell. The hydrophilicity of the core-shell NPs is obviously reduced since their Zeta potential is about  $-4.5$  mV, which is much lower than that of water soluble  $\text{Fe}_3\text{O}_4$  NPs. After mixing the NP solution with toluene, the emulsion droplets can be observed clearly. However, the emulsion droplets were also not stable and phase separation generated after 20 s (see Fig. 2b–e). Therefore, simply tuning the surface charge and hydrophobicity is not enough to achieve stable magnetic colloidosomes.

#### Self-assembly of $\text{Fe}_3\text{O}_4$ - $\text{SiO}_2$ hetero-nanorods at the interface of water-in-oil droplets

In order to make stable magnetic capsules,  $\text{Fe}_3\text{O}_4$ - $\text{SiO}_2$  hetero-nanorods (TEM image shown in Fig. 3a) were employed as building blocks, instead of spherical NPs. In previous studies, we have produced magnetic ( $\text{Fe}_3\text{O}_4$ )-mesoporous ( $\text{SiO}_2$ ) rod-like NPs by using a simple sol-gel method.<sup>33</sup> Such rod-like NPs

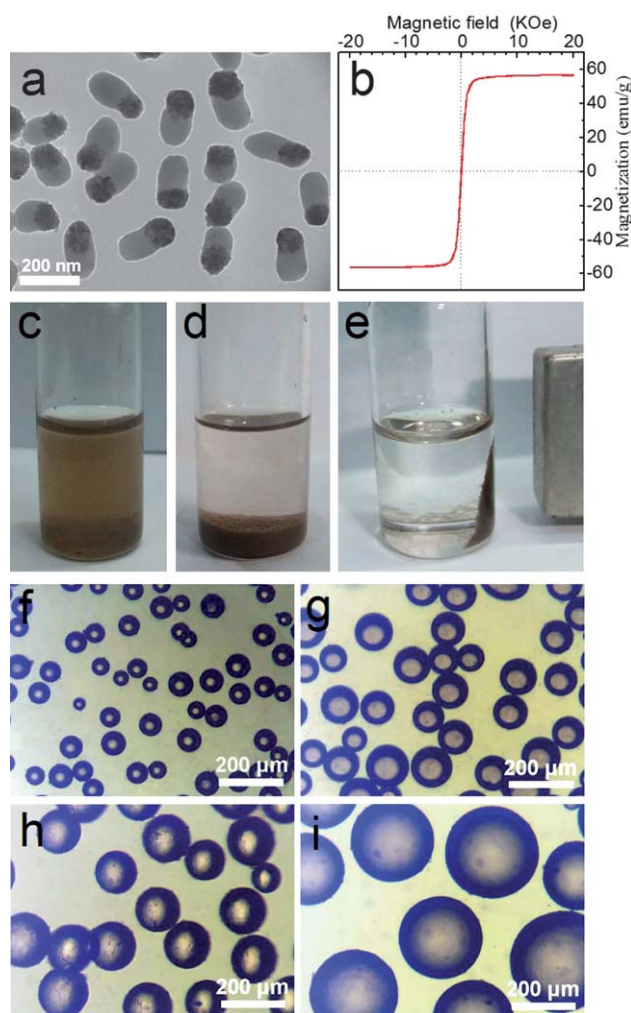


**Fig. 3** TEM image (a) and magnetic hysteresis loop (b) of  $\text{Fe}_3\text{O}_4\text{-SiO}_2$  rod-like NPs with an aspect ratio of 3 : 1. (c–d) Photographs of toluene dispersed magnetic capsules consist of such  $\text{Fe}_3\text{O}_4\text{-SiO}_2$  rod-like NPs. (e) The magnetic colloidosomes were attracted to one side of the vial under an external magnetic field. (f–i) Optical images of magnetic microcapsules with diameter of 60  $\mu\text{m}$  (f), 100  $\mu\text{m}$  (g), 150  $\mu\text{m}$  (h) and 300  $\mu\text{m}$  (i), respectively.

possess not only a high superparamagnetic property but also a regular pore structure. The hetero-nanorods consist of silica sticks and iron NPs. Interestingly, single silica sticks link to individual iron particles and the highly ordered mesoporous structure of rod-like NPs can be clearly observed along the axis of silica body.

The hetero-nanorods in Fig. 3a were prepared with the molar ratio of  $[\text{TEOS} \times 10^{-7}]/[\text{Fe}_3\text{O}_4 \text{ NP}] = 4.9$  in the mixture, with a length-width ratio of 3 : 1 and an average length of approximately 300 nm. The aspect ratio of rod-like NPs would increase as the molar ratio of  $[\text{TEOS} \times 10^{-7}]/[\text{Fe}_3\text{O}_4 \text{ NP}]$  increases. In terms of biological application, the novel anisotropic rod-like NPs appear to be a potentially useful drug carrier because of its stability at physiological pH, peculiar morphology with spatially separated functionalities, and well-defined surface properties for modification. The magnetic property of  $\text{Fe}_3\text{O}_4\text{-SiO}_2$  rod-like NPs was examined by a vibrating sample magnetometer (VSM)

and showed a superparamagnetic behavior with a saturation magnetization of 55  $\text{emu g}^{-1}$  (Fig. 3b) much higher than conventional core-shell particles.<sup>45,46</sup> Crucially, rod-like NPs allow for more drug molecules to load on to their surfaces, which will further increase their stability and allow for better penetration into cells.<sup>47</sup>

The process of preparing microcapsules based on self-assembly of hetero-nanorods at the interface of toluene and the water/ethanol mixture has been illustrated in Scheme 1. A water/ethanol suspension of hetero-nanorods was emulsified in a toluene phase at room temperature. Under severe stirring, the hetero-nanorods oriented themselves at the interface of the two phase and formed magnetic microcapsules in the presence of an organic phase and water phase. Fortunately, such hetero-nanorods were strongly adsorbed at the liquid-liquid interface without homocoagulation and ready to construct stable microcapsules, as shown in Fig. 3c. Because magnetic colloidosomes are too heavy to disperse in the toluene phase, they will rapidly sink to the bottom and encapsulate the aqueous solution inside, (see Fig. 3d). The stability of colloidosomes made by hetero-nanorods is obviously different with that made by spherical core-shell NPs.

The results indicate that the hetero-nanorods may have specific advantages in making stable and coherent shells. However, the Zeta potential of hetero-nanorods was  $-3.8 \text{ mV}$  and very close to that of core/shell particles. Therefore, it is the particle shape effect or the so-called geometric effect which plays an important role in the stability and formation of colloidosomes.

These magnetic colloidosomes have a very strong magnetic response property. As soon as a magnet was applied on one side of the vial, the magnetic microcapsules rapidly moved along the direction of the magnetic field, as shown in Fig. 3. After releasing the magnetic force, gentle shaking led to a rapid redispersion.

From the optical images in Fig. 3f–i, the magnetic colloidosomes are uniform and stable. Their size could also be controlled by adjusting the amount of water. Increasing the water volume, meant the size of the capsules increased but the narrow size distribution was preserved. The size can be facily tuned from 70  $\mu\text{m}$  to 300  $\mu\text{m}$  (Fig. 3f–i).

### “Particle shape” effect

It is well known that the particles are spontaneously adsorbed at the liquids interface if the total free energy of the particles decreases. The behaviour of the rod-like NPs that assemble at the oil/water interface can be explained by the reduction of the interfacial energy.<sup>38,39</sup> The rod-like NPs orient parallel to each other and perpendicular to the plane of the interface to maximize the interfacial coverage per particle, stabilize the water droplets, and minimize the Helmholtz free energy of the system (Scheme 1).<sup>17</sup> The  $\text{Fe}_3\text{O}_4$  head and the  $\text{SiO}_2$  stick were toward the internal aqueous phase and the external oil phase of the emulsion droplets respectively due to the hydrophibility and hydrophobicity discrepancy of the  $\text{Fe}_3\text{O}_4$  end and the  $\text{SiO}_2$  stick end. The contact angle measurement images can be seen in Fig. S1, ESI†. The  $\text{Fe}_3\text{O}_4$  particle is totally hydrophilic, and the contact angle increases to  $19^\circ$  after growing a silica shell. Once the nanoparticle has grown into a rod-like structure, it becomes

more hydrophobic and the contact angle increases to  $25^\circ$ . After all, the rod-like NPs are prone to form stable capsules than spherical (core-shell) particles.

Next, the following question was whether all rod-like NPs can form stable colloidosomes. Thus, the relationship between the optimum aspect ratio of the particles with capsule stability was investigated.  $\text{Fe}_3\text{O}_4\text{-SiO}_2$  hetero-nanorods with different aspect ratios were prepared, as shown in Fig. 3a (aspect ratio of 3 : 1) and Fig. S2, ESI† (aspect ratio of 2 : 1, 4 : 1, 5 : 1 and 7 : 1). We found that the rod-like NPs with aspect ratios of 2 : 1, 3 : 1 and 4 : 1 were facilely used to construct intact and stable magnetic colloidosomes. These hetero-nanorods can migrate to the oil/water interface rapidly and form dense nanoparticle shells, which can stop the coalescence between the magnetic emulsified droplets and stabilize at the water-in-oil emulsion droplets.

However, if the aspect ratio of the rod-like NPs is greater than or equal to 5 : 1, the as-formed colloidosomes become unstable. There were many NPs with an aspect ratio of 5 : 1 in the toluene phase instead of orienting themselves at the interface of two phases (Fig. 4a). Although small colloidosomes can be formed in the toluene phase at the beginning, these colloidosomes will fuse each other into a bigger one (Fig. 4b and c). The fusion phenomenon is mainly due to the low coverage of NPs on the droplet surface so that the coalescence of colloidosomes cannot be prevented efficiently. Finally a large water droplet encapsulated by a nanoparticle shell can be formed in the solution within one month (Fig. 4d).

If the aspect ratio increases to 7 : 1, more NPs can be observed in the toluene phase. Only a few NPs can stay at the oil/water interface and partially cover the droplets. Therefore, the emulsified drops looked like gray wet droplets. The coalescence time between these colloidosomes is strongly reduced. Obviously, the self-assembly of shorter hetero-nanorods at the interface is much easier than the longer ones. The hetero-nanorods with an aspect ratio of 2 : 1, 3 : 1 and 4 : 1 are facile to construct intact and stable magnetic colloidosomes, and 3 : 1 is the optimum aspect ratio.

### Encapsulation and imaging behavior

The encapsulation capability of the magnetic colloidosomes was investigated by confocal laser scanning microscopy (CLSM). Aqueous solutions containing 2.8 nm CdTe NPs were embedded

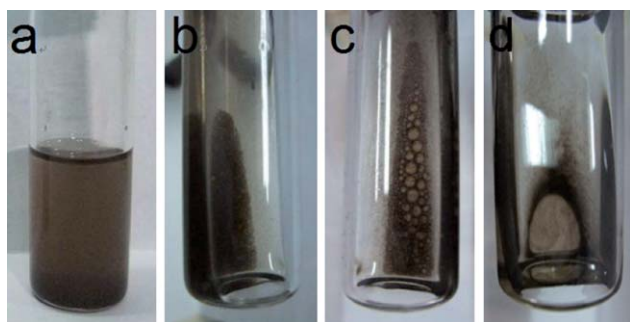


**Fig. 4** Photographs of toluene dispersed magnetic colloidosomes consist of  $\text{Fe}_3\text{O}_4\text{-SiO}_2$  rod-like NPs with an aspect ratio of 5 : 1 (a–d). Small capsules (b) grew into bigger capsules (c) partially until a whole droplet was generated within a month (d).

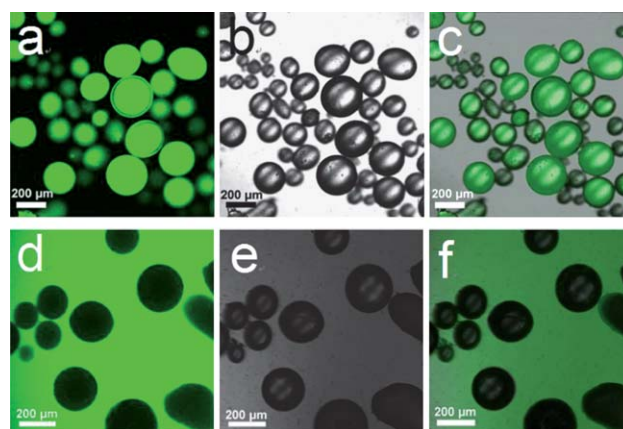


**Fig. 5** (a) Confocal fluorescence microscopy images of magnetic colloidosomes were loaded with 2.8 nm CdTe NPs (a–c) and permeable to porphyrin in toluene (d–f). (a,d) fluorescence images, (b,e) bright-field images, (c,f) merged images).

within magnetic capsules after emulsification. Fig. 5a shows a confocal image of magnetic colloidosomes (hetero-nanorods with an aspect ratio of 3 : 1) loaded with 2.8 nm CdTe NPs with emission at 540 nm, in which the spheres with a homogeneous green emission color are observed. Then, after five times washing with toluene, the shells of the microcapsules remained intact, which indicated that the rod-like NPs were securely fixed at the water/oil interface. The green emission color in the microcapsules could still be observed after a week.

In addition, the integrity of magnetic colloidosomes could be evaluated by adding porphyrin dyes in the toluene phase, followed by observing the fluorescence intensity within the colloidosomes. If the shells of colloidosomes are not intact, the dye will penetrate into the capsules so that the fluorescence can be measured easily. However, after immersing the magnetic colloidosomes in the porphyrin–toluene solution for several days, no fluorescence was observed inside the capsules, as shown in Fig. 5d. As the dye concentration increased, the microcapsules visibly had integrated dark shells seen from CLSM image. Similar results were obtained for other fluorescent dye molecules, which prove the shells of the microcapsules are strongly intact.

Surface modification is another key issue for the utilization of these magnetic-mesoporous rod-like NPs in the field of bio-imaging. Silane coupling agent 3-aminopropyltrimethoxy-silane (APS) was covalently coupled to an amine-reactive dye fluorescein isothiocyanate (FITC).<sup>33</sup> After adding TEOS, 0.03 mL FITC-APS was added to the reaction mixture in the fabrication of rod-like NPs, which didn't disturb the formation and hydrophilicity of the hetero-nanorods. Fig. 6a shows the CLSM images of the fluorescent  $\text{Fe}_3\text{O}_4\text{-SiO}_2\text{-FITC}$  hetero-nanorods. Such fluorescent nanorods could also self-assemble at the two phases to form magnetic capsules. As shown in Fig. 6b, green fluorescence on the outer circle of the capsule can be seen from fluorescent image of the capsules, and Fig. 6c is a bright-field image of the capsules. The as-prepared fluorescent capsules would enable the *in situ* detection and monitoring of the movement of the doped cells under an external magnetic field because of its potential use in bio-separation and related applications.

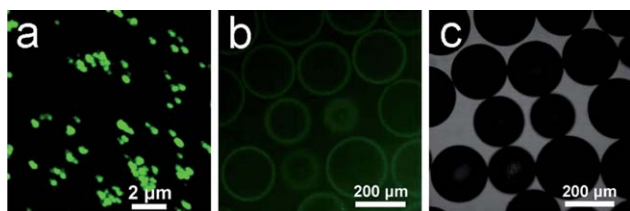


**Fig. 6** (a) Confocal fluorescence microscopy image of FITC labeled  $\text{Fe}_3\text{O}_4\text{-SiO}_2$  hetero-nanorods. Confocal fluorescence microscopy image of magnetic colloidosomes consists of rod-like NPs with an aspect ratio of approximately 3 : 1, (b) fluorescence image, (c) bright-field image.

The as-resulting magnetic colloidosomes contain the aqueous solution and disperse in the toluene phase. How to transfer them to the water phase was another key issue for their further application. Herein, we also demonstrated that agarose hydrogel can be effectively encapsulated in the magnetic colloidosomes. The hydrogel-loaded magnetic colloidosomes can be easily transferred into the aqueous phase, as shown in Fig. S3, ESI†. Obviously, these novel colloidosomes would be regarded as biocompatible carriers for drug loading and controlled release.

### Magnetic manipulation behavior

Magnetic properties of the colloidosomes play an important role in the field of biomedical science and technology. The magnetic-direct assembly properties of magnetic colloidosomes were studied under an external magnetic field. Herein, magnetic colloidosomes with a diameter of 60  $\mu\text{m}$  were chosen for further investigation. A droplet of toluene solution containing the magnetic colloidosomes was placed on a square groove. Subsequently, a permanent magnet was placed close to one side of the groove with the magnetic line of force running parallel with the groove plane. As shown in Fig. 7, the colloidosomes aligned into one-dimensional necklace-like structures under the magnetic field. This is mainly due to the dipole-dipole interactions between the adjacent magnetic colloidosomes which can couple themselves together and force the formation of anisotropic structures. Such high magnetic sensitivity and manipulability of colloidosomes may have great potential in manipulation and organization of magnetic structures into integrated system.<sup>48</sup>

Moreover, the emulsion stability of the magnetic colloidosomes under magnetic manipulation was studied by evaluating the time-resolved integrity of the magnetic microcapsules. Here, the CLSM was used to investigate the changes of the capsule

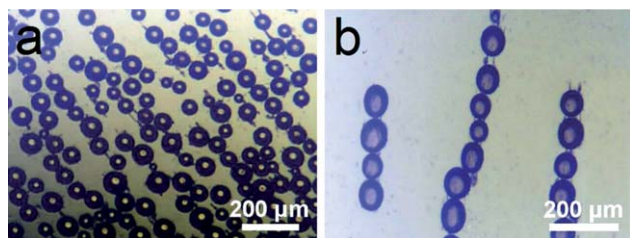


**Fig. 7** (a) Optical images of magnetic colloidosomes under an external magnetic field. (b) A straight chain of magnetic microcapsules aligned by an external magnetic field.

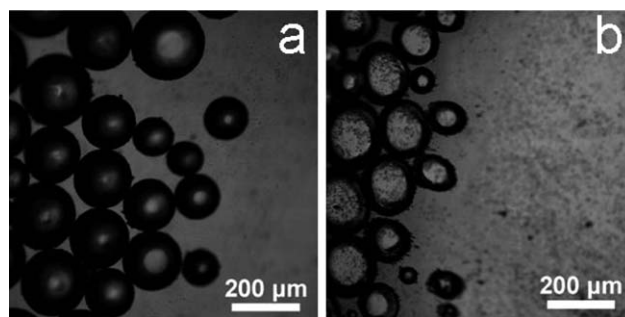


**Fig. 8** CLSM image of magnetic colloidosomes consisting of rod-like NPs with an aspect ratio of approximately 3 : 1 under the application of a magnet with measurement time of 10 s (a) and 60 min (b).

integrity and the magnitude of the magnetic force was controlled by adjusting the distance between the magnet and the sample. After placing the magnet by the groove, all the magnetic colloidosomes were attracted to one side of small groove. The size and shape of magnetic colloidosomes did not change at the beginning of 10 s (Fig. 8a). However, after 60 min (Fig. 8b), the shape of the colloidosomes started to change a little bit. Moreover, just a few magnetic particles had been deflected by the long-term magnetic force. The results not only reveal the excellent emulsion stability of magnetic colloidosomes made by hetero-nanorods, but also demonstrate the superior mechanical stability of nanoparticle films on the oil/water interface.

### Conclusions

In this work, novel multifunctional magnetic colloidosomes were fabricated by directing the self-assembly of  $\text{Fe}_3\text{O}_4\text{-SiO}_2$  hetero-nanorods at the interface of water-in-oil droplets. Emulsions stabilized by the adsorbed particles without any surfactant indicated that such rod-like NPs have specific advantages in making stable and coherent shells than spherical particles. Besides the effects of surface charge and hydrophobicity, the particle shape effect plays an important role in the preparation of stable colloidosomes. The optimum aspect ratio of hetero-nanorods falls within the range of 2 : 1 to 4 : 1 which results in high yielding, intact and stable magnetic colloidosomes. These as-forming microcapsules have unique encapsulation properties for numerous materials, for instance, dyes, quantum dots or biomacromolecules. Due to their special magnetic responsibility, these colloidosomes can be easily manipulated and self-aligned under an external magnetic field, which can find potential applications in microreactor, drug delivery and other biomedical fields.

### Acknowledgements

This work is supported by the National Science Foundation of China (Grant Nos. 60977056, 61077066, 60978062 and 90923037).

### References

- 1 I. Cohen, H. Li, J. L. Hougland, M. Mrksich and S. R. Nagel, *Science*, 2001, **292**, 265.

- 2 I. G. Loscertales, A. Barrero, I. Guerrero, R. Cortijo, M. Marquez and A. M. Gañán-Calvo, *Science*, 2002, **295**, 1695.
- 3 T. Joki, M. Machluf, A. Atala, J. H. Zhu, N. T. Seyfried, L. F. Dunn, T. Abe, R. S. Carroll and P. M. Black, *Nat. Biotechnol.*, 2001, **19**, 35.
- 4 Y. J. Ma, W. F. Dong, M. A. Hempenius, H. Möhwald and G. J. Vancso, *Nat. Mater.*, 2006, **5**, 724.
- 5 J. K. Kim, E. Lee, Y. B. Lim and M. Lee, *Angew. Chem., Int. Ed.*, 2008, **47**, 4662.
- 6 J. Jang and K. Lee, *Chem. Commun.*, 2002, 1098.
- 7 S. Benita, *Microencapsulation: Methods and Industrial Applications*, 2nd ed.; CRC Press: Boca Raton, FL, 2006.
- 8 F. Tiarks, K. Landfester and M. Antonietti, *Langmuir*, 2001, **17**, 908.
- 9 H. Oana, A. Kishimura, K. Yonehara, Y. Yamasaki, M. Washizu and K. Kataoka, *Angew. Chem., Int. Ed.*, 2009, **48**, 4613.
- 10 F. Caruso, *Top. Curr. Chem.*, **227**, 145.
- 11 C. C. Deng, W. F. Dong, T. Adalsteinsson, J. K. Ferri, G. B. Sukhorukov and H. Möhwald, *Soft Matter*, 2007, **3**, 1293.
- 12 A. D. Dinsmore, M. F. Hsu, M. G. Nikolaides, M. Marquez, A. R. Bausch and D. A. Weitz, *Science*, 2002, **298**, 1006.
- 13 O. D. Velev and K. Nagayama, *Langmuir*, 1997, **13**, 1856.
- 14 H. W. Duan, D. Y. Wang, N. S. Sobal, M. Giersig, D. G. Kurth and H. Möhwald, *Nano Lett.*, 2005, **5**, 949.
- 15 Y. Xia, B. Gates, Y. Yin and Y. Lu, *Adv. Mater.*, 2000, **12**, 693.
- 16 C. Zeng, H. Bissig and A. D. Dinsmore, *Solid State Commun.*, 2006, **139**, 547.
- 17 G. M. Whitesides and B. Grzybowski, *Science*, 2002, **295**, 2418.
- 18 S. Murthy, J. N. Cha, G. D. Stucky and M. S. Wong, *J. Am. Chem. Soc.*, 2004, **126**, 5292.
- 19 Y. Zhang, Y. F. Wu, M. Chen and L. M. Wu, *Colloids Surf., A*, 2010, **353**, 216.
- 20 S. B. Yang, H. H. Song, H. X. Yi, W. X. Liu, H. J. Zhang and X. H. Chen, *Electrochim. Acta*, 2009, **55**, 521.
- 21 A. Böker, J. B. He, T. Emrick and T. P. Russell, *Soft Matter*, 2007, **3**, 1231.
- 22 X. Li, X. Li, J. Zhang, S. Zhao and J. Shen, *J. Biomed. Mater. Res., Part A*, 2008, **85A**, 768.
- 23 O. P. Tiourina and G. B. Sukhorukov, *Int. J. Pharm.*, 2002, **242**, 155.
- 24 H. Gharapetian, M. Maleki, G. M. O'Shea, R. C. Carpenter and A. M. Sun, *Biotechnol. Bioeng.*, 1987, **30**, 775.
- 25 J. P. Wong, L. L. Stadnyk and E. G. Saravolac, *Immunology*, 1994, **81**, 280.
- 26 Y. J. Wang, Y. Yan, J. W. Cui, L. Hosta-Rigau, J. K. Heath, E. C. Nice and F. Caruso, *Adv. Mater.*, 2010, **22**, 4293.
- 27 B. G. D. Geest, G. B. Sukhorukov and H. Möhwald, *Expert Opin. Drug Delivery*, 2009, **6**, 613.
- 28 G. B. Sukhorukov, A. L. Rogach, M. Garstka, S. Springer, W. J. Parak, A. Muñoz-Javier, O. Kreft, A. G. Skirtach, A. S. Susa, Y. Ramaye, R. Palankar and M. Winterhalter, *Small*, 2007, **3**, 944.
- 29 W. Wang, X. D. Liu, Y. B. Xie, H. A. Zhang, W. T. Yu, Y. Xiong, W. Y. Xie and X. J. Ma, *J. Mater. Chem.*, 2006, **16**, 3252.
- 30 N. Zhao and M. Y. Gao, *Adv. Mater.*, 2009, **21**, 184.
- 31 B. Samanta, D. Patra, C. Subramani, Y. Ofir, G. Yesilbag, A. Sanyal and V. M. Rotello, *Small*, 2009, **5**, 685.
- 32 J. P. Ge, Y. X. Hu, M. Biasini, W. P. Beyermann and Y. D. Yin, *Angew. Chem., Int. Ed.*, 2007, **46**, 4342.
- 33 L. Zhang, F. Zhang, W. F. Dong, J. F. Song, Q. S. Huo and H. B. Sun, *Chem. Commun.*, 2011, **47**, 1225.
- 34 H. Xia, L. Zhang, Q. D. Chen, L. Guo, H. H. Fang, X. B. Li, J. F. Song, X. R. Huang and H. B. Sun, *J. Phys. Chem. C*, 2009, **113**, 18542.
- 35 L. Zhang, W. F. Dong, Z. Y. Tang, J. F. Song, H. Xia and H. B. Sun, *Opt. Lett.*, 2010, **35**, 3297.
- 36 J. P. Ge and Y. D. Yin, *Adv. Mater.*, 2008, **20**, 3485.
- 37 B. P. Binks and P. D. I. Fletcher, *Langmuir*, 2001, **17**, 4709.
- 38 C. Ybert, W. Lu, G. Möller and C. M. Knobler, *J. Phys. Chem. B*, 2002, **106**, 2004.
- 39 Q. Chen, J. K. Whitmer, S. Jiang, S. C. Bae, E. Luijten and S. Granick, *Science*, 2011, **331**, 199.
- 40 P. F. Noble, O. J. Cayre, R. G. Alargova, O. D. Velev and V. N. Paunov, *J. Am. Chem. Soc.*, 2004, **126**, 8092.
- 41 O. D. Velev, K. Furusawa and K. Nagayama, *Langmuir*, 1996, **12**, 2374.
- 42 L. X. Yi, A. W. Tang, M. Niu, W. Han, Y. B. Houb and M. Y. Gao, *CrystEngComm*, 2010, **12**, 4124.
- 43 F. H. Stillinger, *J. Chem. Phys.*, 1961, **35**, 1584.
- 44 P. Pieranski, *Phys. Rev. Lett.*, 1980, **45**, 569.
- 45 W. R. Zhao, J. L. Gu, L. X. Zhang, H. R. Chen and J. L. Shi, *J. Am. Chem. Soc.*, 2005, **127**, 8916.
- 46 H. M. Chen, C. H. Deng and X. M. Zhang, *Angew. Chem., Int. Ed.*, 2010, **49**, 607.
- 47 A. C. Bonoiu, S. D. Mahajan, H. Ding, I. Roy, K. T. Yong, R. Kumar, R. Hu, E. J. Bergey, S. A. Schwartz and P. N. Prasad, *Proc. Natl. Acad. Sci. U. S. A.*, 2009, **106**, 5546.
- 48 M. Motornov, Y. Roiter, I. Tokarev and S. Minko, *Prog. Polym. Sci.*, 2010, **35**, 174.